Synthesis, Characterization and DNA Binding Studies of N,N′-*bis*(2-Hydroxy-5-methyl-benzylidene)-2-hydroxy-propane-1,3-diamine Copper(II) and Nickel(II) Complexes

RAMINA[1], RAJKUMAR BHUBON SINGH[1,*], OINAM U-WANG[1], THOUDAM SURCHANDRA SINGH[1] and T. TIAKABA JAMIR[2]

[1]Department of Chemistry, Manipur University, Canchipur-795003, India
[2]Department of Chemistry, Kohima Science College, Kohima-797002, India

*Corresponding author: E-mail: bhubonsingh@gmail.com

Two new Schiff base transition metal complexes [Cu(HL)]₂.CH₃CH₂OH (**1**) and [Ni(HL)] (**2**) (L = N,N′-*bis*(2-hydroxy-5-methyl-benzylidene)-2-hydroxy-propane-1,3-diamine) were synthesized and characterized by different physico-chemical and spectroscopic techniques. Structure of complex **1** was determined by single crystal X-ray diffractometer. Both the complexes have distorted square planar geometry. The DNA binding study of two complexes was performed *via* electronic absorption, cyclic voltammetry, photoluminescence, and viscosity methods and found to be intercalative mode of binding.

Keywords: Schiff base, Cu(II) and Ni(II) complexes, DNA binding.

INTRODUCTION

Nowadays interests in Schiff bases of diamine having an alcoholic group in the backbone have been brought due to the maximal possibility in design and synthesis of novel and unusual homo as well hetero-polynuclear coordination compounds [1-3]. Schiff bases of salen type have been encountered to possess a number of biological applications namely antibacterial, antifungal, antioxidant and oxygen carrier activities. These properties are more in metal complexes as compared to non-complexing ligand [4-6]. It has also been reported that Schiff base of type N,N′-*bis*(5-bromo-salicylidene)-2-hydroxy-1,3-propane diamine (BSHP) used as an alternative analytical method for the iron determination in oils [7].

One more exciting example was in Mn(III) Schiff base complex of 2-hydroxybenzaldehyde and 1,3-diamino-2-hydroxypropane, which have more efficacy as compared to its analogues 1,3-diaminopropane towards oxidation of a different kind of olefins. It has attributed to accompany of an electron-withdrawing group -OH in the amine [8]. Besides, this type of amine also offers the formation of macrocycles with suitable carbonyl compounds mainly phenol-based to insulate *f*- or *s*-block metal ions over transition metal ions to model heteronuclear compounds [9]. Having properties like magnetic materials,

catalysts and models for metalloenzymes [10-13] also brought the room in the selective designation of complexes of such kind of macrocyclic Schiff bases. Some of these herein mention because of such ligands can act as flexible chelators towards metal ions that is, it can be tribasic pentadenate, dibasic tetra-dentate or tridentate ligands. Such flexibility is possible with the involvement or abstention of the secondary hydroxyl group and one of two parts of the Schiff base [14,15]. Therefore, it is notable the pentadentate chelating octahedral polymeric *zig-zag* chain copper(II) complex having [CuL] as monomeric unit [16], where, L = [N,N′-*bis*(4-methoxysalicylidene)-2-hydroxy-1,3-diaminopropane]. Also, monomeric tetrachelated octahedral vanadium(IV) complex [V^{IV}O(Hsal-dahp)(DMSO)] and pentacoordinated polymer-supported vanadium(IV) complex PS-[V^{IV}O(sal-dahp)], which shows peroxidase-like activity in oxidation of pyrogallol to purpurogallin (PS = chloromethylated polystyrene cross-linked with 5% divinylbenzene and H₃sal-dahp = tribasic pentacoordinate ligand obtained from 2-hydroxy-benzaldehyde and 2-hydroxy-1,3-propanediamine) [17]. Again, vanadium(V) complexes [V^{V}O(hap-dahp)] and [V^{V}O-(hap-dahp)]-Y with H₃hap-dahp (where, H₃hap-dahp = Schiff base synthesized from 2-hydroxy acetophenone and 1,3-diamino-2-hydroxypropane) and its catalytic activity in oxida-tion of vinylbenzene, thioanisole and phenyl sulfide with H₂O₂

as an oxidant of these pentadentate octahedral could be high-light [18]. Along with dibasic tridentate octahedral complexes [Mo^{VI}O$_2$(Hsal-dahp)-(H$_2$O)], [Mo^{VI}O$_2$(Hclsal-dahp)-(H$_2$O)] and [Mo^{VI}O$_2$(Hbrsal-dahp)-(H$_2$O)], which shows catalytic activity towards oxidative bromination of vinyl benzene to give (1,2-dibromoethyl)benzene, styrene glycol and styrene bromohydrin could be given [14]. It has also proclaimed that the *d*-block metal complexes were biological effectiveness towards DNA binding and cleavage [19].

From the literature study, synthesis of Schiff base ligand, {N,N′-*bis*(2-hydroxy-5-methyl-benzylidene)-2-hydroxy-propane-1,3-diamine} and its metal complexes have been found [20]. To continue the work of our group [21-25] on the synthesis, characterization and DNA binding studies of transition metal complexes, we herein report a new copper (II) and Ni(II) complexes synthesized by a template method and their characterization by different spectroscopic techniques along with CT-DNA binding studies of the complexes.

EXPERIMENTAL

1,3-Diamino-2-hydroxy-propane, 5-methyl-salicylaldehyde, metal chlorides or nitrates and solvents were obtained from Sigma-Aldrich, Merck, Himedia. CT-DNA and Tris-HCl (biological grade) were obtained from Himedia and used as received. Carbon, hydrogen and nitrogen analyses were recorded on a Perkin-Elmer 2400-II elemental analyzer. IR spectra were recorded on a Perkin-Elmer FTIR 400 spectrophotometer within the scale of 4000-400 cm^{-1} by employing KBr pellets. Electronic spectra were recorded on a Shimadzu UV-Visible 2450 Spectrophotometer. On Sherwood magnetic susceptibility balance (MSB), magnetic susceptibility measurement was performed using CuSO$_4$·5H$_2$O as the standard substance at room temperature. Pascal′s constants were applied to made diamagnetic corrections. Simultaneous TGA and DTA were recorded by using Perkin-Elmer STA 6000 Simultaneous thermal analyzer at a heating rate of 10 ºC per minute under nitrogen atmosphere. Molar conductivity was measured at 25 ºC in DMSO (10^{-3} mol L^{-1}) by using Eutech Con 510 conductometer. Powder XRD of complex **2** was measured by using a PAN-analytical Philips diffractometer. Cyclic Voltammetry measurements were performed using a CH602C Electrochemical Analyzer against the AgNO$_3$/Ag reference electrode. The mass spectrum of complex **2** has measured using Waters (ZQ-4000) (ESI-MS) spectrometer. The fluorescence measurements were conducted on F-7000 FL Spectrophotometer along with excitation as well as emission slit widths (5 nm). The viscosity of complexes was measured by using Ostwald′s viscometer.

Synthesis of metal(II) complexes: Ethanolic solutions of 1,3-diamino-2-hydroxypropane (1 mmol, 0.0901 g) (10 mL) and 5-methyl-salicylaldehyde (2 mmol, 0.2723 g) (10 mL) were refluxed for about 2 h to give yellow-orange colouration. To this solution mixture, copper(II) nitrate trihydrate (1 mmol, 0.2416 g) in 10 mL ethanol was added and continued to reflux for another 4 h in the presence of triethylamine (3 mmol, 0.417 mL). Then, filtered and the filtrate was kept for slow evaporation at room temperature. After two weeks, dark green needle shaped single-crystals of complex **1** suitable for X-ray crystal-

lography were collected from the filtrate. Similarly, complex **2** was also synthesized using nickel(II) chloride hexahydrate (1 mmol, 0.237 g) (**Scheme-I**).
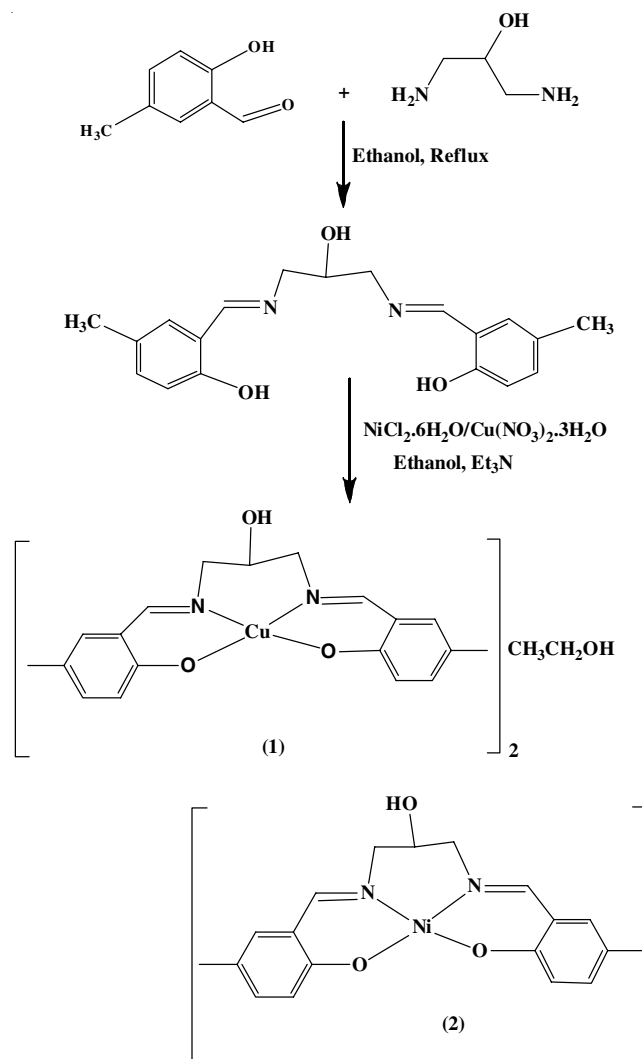
Scheme-I: Reaction pathways for complexes (**1**) and (**2**)

[Cu(HL)]$_2$·C$_2$H$_5$OH (**1**): Yield: 75.81%, dark green, m.p.: 292 ºC, m.w.: 821.89; Anal. calcd. (found) (%): Cu, 15.33 (15.43); C, 58.40 (58.45); H, 5.59 (5.50); N, 6.81 (6.78); UV-Vis (λ_{max}) (DMSO): 612 nm; IR (KBr, ν_{max}, cm^{-1}): 3217 (O-H), 3014 (Ar-CH), 2920 (methyl-CH), 2862 (aldehydic-CH), 1631 (C=N) and 1219 (C-O), 418 (Cu-N), 501 (Cu-O); molar conductance (DMSO): 6.3 Ω^{-1}cm^2 mol^{-1}; μ_{eff} (B.M):1.26.

[Ni(HL)] (**2**): Yield: 76.45%, yellow, m.p.: 275 ºC, m.w.: 382; Anal. calcd. (found) (%): Ni, 15.18 (15.05); C, 59.68 (59.98); H, 5.23 (5.04); N, 7.32 (7.12); UV-Vis (λ_{max}) (acetonitrile): 590 nm; IR (KBr, ν_{max}, cm^{-1}): 3367 (O-H), 3012 (Ar-CH), 2920 (methyl-CH), 2864 (aldehydic-CH), 1624 (C=N) and 1224 (C-O), 422 (Cu-N), 526 (Cu-O); molar conductance (DMSO): 2.61 Ω^{-1}cm^2 mol^{-1}; μ_{eff} (B.M): diamagnetic.

Crystallographic data collection and refinement: Intensity data of complex **1** was collected on a Bruker AXS Kappa Apex 3 CMOS single-crystal X-ray diffractometer by using the graphite monochromated Mo-Kα radiation (λ = 0.71073 Å at 296 K).

SHELXT-2014/5 was applied to solve the structure and SHELXL-2014/7 to refine the structure [26]. A full-matrix least-squares procedure was applied to refine the structure which carried out on F^2. Non-hydrogen atoms were assigned anisotropic displacement parameters. Hydrogen atoms were at their absolute locations using isotropic displacement parameters. The crystallographic data for complex **1** is shown in Table-1, while the molecular structure as well as packing structure diagram is shown in Figs. 1 and 2, respectively by OLEX-2 [27]. Some selected bond lengths, as well as angles for complex **1** are shown in Table-2.

TABLE-1 FOR COMPLEX (**1**) CRYSTAL STRUCTURAL DATA AND ITS REFINEMENT	
Empirical formula	$C_{40}H_{46}N_4O_7Cu_2$
Formula weight (g mol^{-1})	821.89
Temperature (K)	296(2)
Crystal system	Monoclinic
Space group	P2$_1$/c
Unit cell dimensions	a = 12.0389(6) Å; α = 90°
	b = 10.4997(5) Å; β = 110.396(2)°
	c = 16.0395(8) Å; γ = 90°
	1900.36 (16)
Volume (Å^3)	2
Z	1.436
Density (calculated) (Mg/m^3)	1.174
Absorption coefficient (mm^{-1})	3.250-24.993
θ range for data collection (°)	-14 ≤ h ≤ 14, -12 ≤ k ≤ 12, -19 ≤ l ≤
Index ranges	19
Reflections collected	29507
Independent reflections	3345 [R(int) = 0.0878]
Data/restraints/parameters	3345/16/265
Goodness-of-fit on F^2	1.049
R indices (all data)	R1 = 0.1214, wR2 = 0.2152
Largest difference in peak and hole	0.848 and -0.782 (e. Å^{-3})

DNA binding studies: To know the interaction mode of the newly synthesized complexes to CT-DNA, electronic absorption titration, fluorescence experiment, cyclic voltammetry, and viscosity measurements have been performed.

RESULTS AND DISCUSSION

The complexes **1** and **2** were synthesized according to (**Scheme-I**) *via* the template methodology. Characterizations of these complexes have been performed by different spectroscopic techniques. Complex **1** is soluble in DMSO, DMF while partially soluble in methanol, ethanol and acetonitrile. Whereas, complex **2** is soluble in almost all organic solvents. From the
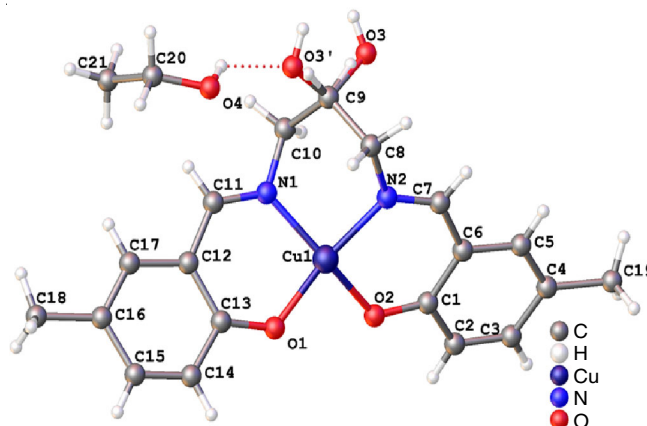

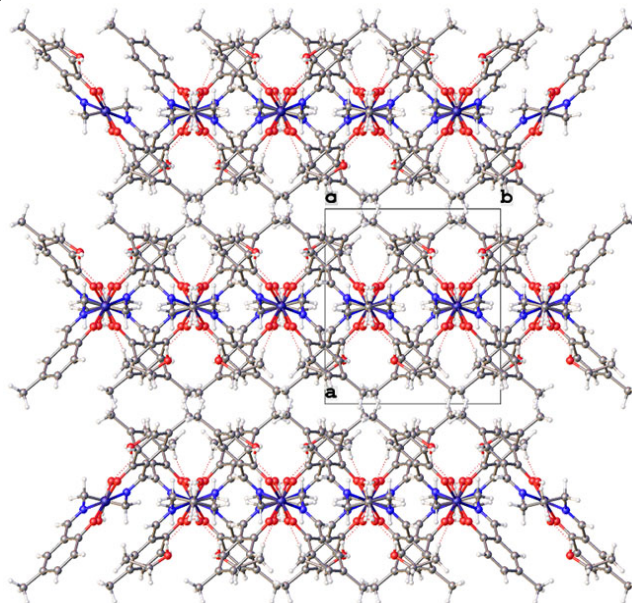Fig. 1. Molecular structure of complex (**1**) with atoms numbering scheme

Fig. 2. Packing structure for complex (**1**) showing the possibility of hydrogen-bonding along the c-axis

molar conductance data, reckons a non-electrolyte type in the DMSO [28]. All the complexes are non-hygroscopic.

IR analysis: IR spectrum of complex **1** shows the presence of main functional groups. Bands observed at 3217, 3014, 2920, 2862, 1631, and 1219 cm^{-1} may be assigned to ν(O-H), ν(C-H), ν(C=N) and ν(C-O) stretching vibrations of alcoholic, aryl, methyl, aldehydic, azomethine and phenyl ring, respectively [29-33]. Further, bands observed at 418 and 501 cm^{-1} may be assigned to ν(M-N) and ν(M-O) stretching vibrations, respectively [34,35].

TABLE-2 SOME SELECTED BOND LENGTHS (Å) AND ANGLES (°) FOR (**1**)					
Bond length	Å	Bond angle	°	Bond angle	°
Cu1–O1	1.903(5)	O1–Cu1–N1	94.7(2)	O2–Cu1–N2	94.5(2)
Cu1–O2	1.901(5)	O2–Cu1–O1	91.9(2)	C11–N1–Cu1	125.3(5)
Cu1–N1	1.936(6)	O1–Cu1–N2	153.2(2)	C10– N1–Cu1	115.2(5)
Cu1–N2	1.942(6)	O2–Cu1–N1	153.4(2)	C7–N2–Cu1	125.1(5)
C11-N1	1.281(9)	N1–Cu1–N2	91.1(2)	C8–N2–Cu1	114.9(5)
C7-N2	1.272(9)	C13–O1–Cu1	125.8(4)	C1–O2–Cu1	126.1(4)

Symmetry codes: (i) x, y, z; (ii) -x, y+1/2, -z+1/2; (iii) -x, -y, -z; (iv) x, -y-1/2, z-1/2.

The vibrational absorption spectrum of complex **2** shows the presence of stretching vibration of alcoholic ν(O-H) at 3367 cm⁻¹. Additional ν(C-H) stretching vibrations of aryl, methyl and aldehydic appears at 3014, 2920 and 2864 cm⁻¹, respectively. Bands at 1624 and 1224 cm⁻¹ have been assigned to ν(C=N) and ν(C-O) stretching vibrations of azomethine and phenyl ring, respectively. The ν(M-N) and ν(M-O) stretching bands were observed at 422 and 526 cm⁻¹.

Electronic absorption analysis: UV-vis spectrum of complex **1** was recorded in DMSO (10⁻³ mol L⁻¹). A broad *d-d* band observed at 612 nm could be assigned at the transition of $^2B_{1g} \rightarrow {}^2A_{1g}$ of a distorted square planar structure [36,37]. Whereas, complex **2** recorded in acetonitrile (10⁻³ mol L⁻¹) exhibit a *d-d* band at 590 nm, which may be assigned to $d_{xy} \rightarrow d_{x^2-y^2}$ of distorted square planar geometry [38].

Mass analysis: ESI-MS technique has been employed to see the molecular mass of the complex. Molecular ion peak of complex **2** appeared at *m/z* value = 382 is in good agreement with theoretically calculated mass. Additional information comes from the main fragmentations with *m/z* values equal to 276(274) and 242, 243. The mass spectrum of complex **2** (Fig. 3) along with its plausible fragmentation pattern is shown in Fig. 4.

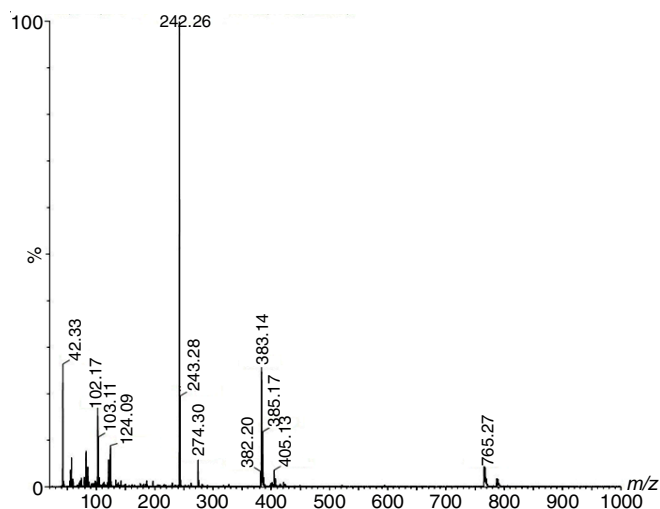Fig. 4. Mass fragmentation pattern of complex (**2**)

Fig. 3. Mass spectrum of [Ni(HL)] (**2**) complex

Powder-XRD analysis: In complex [Cu(HL)]₂·C₂H₅OH (**1**), the empirical formula is fulfilled by two [Cu(HL)] neutral monomeric units and one lattice ethanol molecule. In the monomer unit, Cu(II) ion is coordinated by two azomethine N atoms and two phenolate O atoms of the Schiff base ligand leaving aside O donor atom of the alcoholic group in a six-membered chelating fashion. The equatorial plane of coordination sphere are filled by the ONNO chromophore having average bond distances of Cu(1)-O(1) = 1.903 Å, Cu(1)-N(1) = 1.936 Å, Cu(1)-N(2) =1.942 Å and Cu(1)-O(2) = 1.901 Å. There are hardly differences in between Cu-N_imine atoms (0.006 Å) or Cu-O_phenoxo atoms (0.002 Å) but a slightly longer of Cu-N_imine bonds than Cu-O _phenoxo bonds have been observed. It is found that angles around the metal centre have deviated from the ideal value 90º of a regular square planar geometry for all [N(1)-Cu(1)-N(2): 91.1(2)º, N(1)-Cu(1)-O(1): 94.7(2)º, O(1)-Cu(1)-O(2): 91.9(2)º,

O(2)-Cu(1)-N(2): 94.5(2)º]. The amount of deviation from this equatorial plane [O(1)-N(1)-N(2)-O(2)] could be determined by using the structural parameter (τ) [39-41]. Values of τ₄ (0.378) and τ₄₂ (0.377) indicates a distorted square planar structure and crystallized in a monoclinic system of space group P2₁/c. The N=CH bond distances [N(1)-C(11): 1.281(9) Å and N(2)-C(7): 1.272(9) Å] are constant with C=N double bonds character, the C-O bonds [C(13)-O(1):1.314(9) Å, C(1)-O(2): 1.317(8) Å and C(9)-O(3):1.451(9) Å] as well as C-N bonds [C(10)-N(1): 1.456(8) Å and C(8)-N(2):1.459(9) Å] also consistent in a single bond behaviour. Two positive charges of Cu(II) ions have been neutralized by two phenoxo groups. It was also in good agreement with the conductance value. The torsion angles of the planes containing C(17)-C(12)-C(11)-N(1), C(5)-C(6)-C(7)-N(2), C(15)-C(14)-C(13)-O(1), C(3)-C(2)-C(1)-O(2), C(17)-C(12)-C(13)-O(1) and C(5)-C(6)-C(1)-O(2) found to be 176.7 (7), 174.4(7), -174.4(7), -174.7(7), 174.4(7) and 173.4(6)º, respectively . All values were found to be close at 180º. It was viewed to develop one dimensional hydrogen bonding in the crystal packing of complex **1** *via* the hydrogen atom H(3A) attached to alcoholic oxygen (O3) of carbon (C9) of one monomer unit and phenoxo oxygen (O2) attached to carbon (C1) of another neighbouring monomer unit along with the O3-H3A and H3A-O2 bond lengths equal to 0.82 and 1.9 Å, respectively. Further, the lattice ethanol molecule is also participating in the hydrogen bonding.

The diffraction pattern of complex **2** is given in Fig. 5. Unit cell parameters were produced using the program P-index and found to be triclinic. Unit cell parameters are a = 7.6095, b = 7.7058, c = 13.2336 Å, α = 40.105º, β = 136.715º, γ = 144.989º and V = 275.77 Å³. Crystallite size of the complex, d_xrd was evaluated using the Debye-Scherrer's formula [42]. d_xrd = 0.9 λ/βcos θ. Where β meant full width at half maximum of the prominent peak, θ is the Braggs reflection angle, and λ is the wavelength of Cu*K*α radiation (1.5406 Å). The calculated average crystallite size is 35.9 nm and falls in the nano-range.
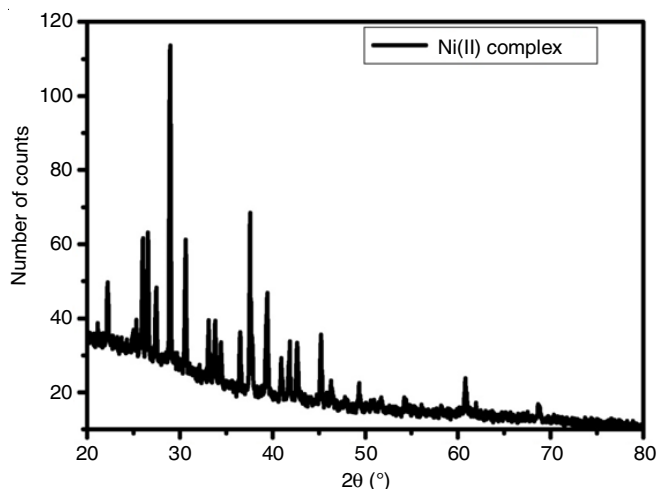
Fig. 5. PXRD pattern of [Ni(HL)] complex (**2**)

Thermal analysis: Thermograms of complexes **1** and **2** are shown in Figs. 6 and 7, respectively. The first decomposition step of complex **1** has shown in the temperature range of 135-219 ºC showing the removal of one ethanol molecule followed by decomposition of one ligand in the temperature range of 281-880 ºC. Whereas, complex **2** has shown stable up to 296 ºC and start decomposition in one step in the temperature range of 297-843 ºC showing the expulsion of the ligand molecule.
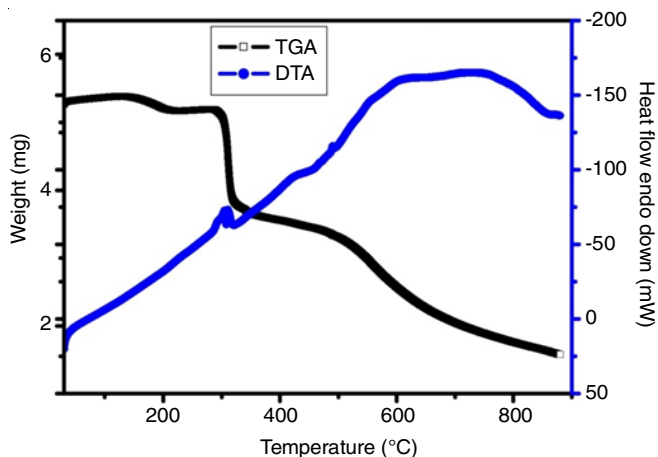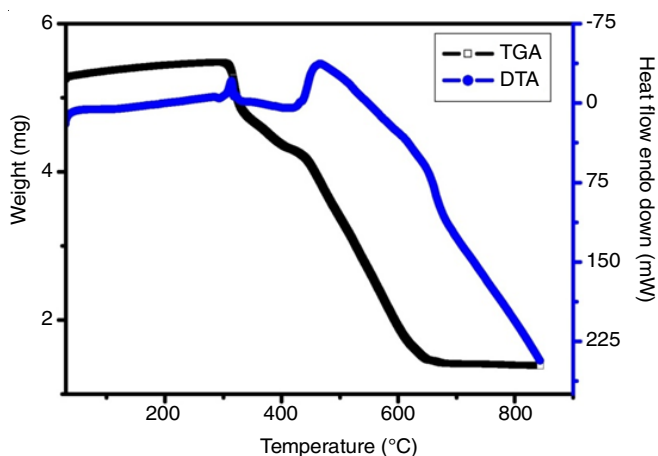

Fig. 6. TGA-DTA graph of complex **1**

Fig. 7. TGA-DTA graph of complex **2**

DNA binding studies of complexes 1 and 2

Absorption spectral method: DNA binding studies were carried out in *tris*-HCl buffer which composed of 5 mM *tris*-HCl and 50 mM NaCl (pH = 7.2) along with a CT-DNA solution in a suitable volume of this buffer. The ratio of absorbance peaks at 260 and 280 nm is about 1.8-1.9, indicates the DNA was sufficiently free from protein. The DNA concentration also calculated using the known value, 6600 M^{-1} for the molar absorptivity coefficient at 260 nm. Absorption titration was carried out at a definite complex concentration by changing the DNA concentration in the buffer. Solution of metal complexes in DMSO was employed, on account of poor solubility in other solvents. The intrinsic binding constant, K_b was evaluated from the following equation:

$$\frac{[DNA]}{(\varepsilon_a - \varepsilon_f)} = \frac{[DNA]}{(\varepsilon_b - \varepsilon_f)} + [K_b(\varepsilon_b - \varepsilon_f)]^{-1} \qquad (1)$$

In the equation, [DNA] is the DNA concentration in base pairs, ε_a, ε_f and ε_b indicates apparent, free and bound metal complexes extinction coefficients respectively, K_b represents the ratio of the slope to the intercept by plotting $[DNA]/(\varepsilon_a - \varepsilon_f)$ *versus* [DNA] [43]. To support, the interaction of metal complexes with CT-DNA, an absorption titration technique was employed. Transition metal complexes have been found to bind to DNA *via* both covalent and/or non-covalent interaction [44]. An intercalation mode shows a trend of intensity decreasing (hypochromism) with or without the red/blue shift (Figs. 8 and 9) [45]. Both the complexes have shown a similar behaviour that is, with increasing CT-DNA concentration, the intra-ligand bands at 364 and 348 nm for complexes **1** and **2**, a decrease in absorption intensity without any significant shift. It implies that there is an association among the complexes and DNA. K_b values are found to be 0.98×10^4 and $0.41 \times 10^5\,M^{-1}$, respectively for complexes **1** and **2**. Thus, the present K_b values fall nearly to (1.116-7.227) of order (10^4) [46,47] as compared to the value of classical intercalator, EB ($1.4 \times 10^6\,M^{-1}$) [48].
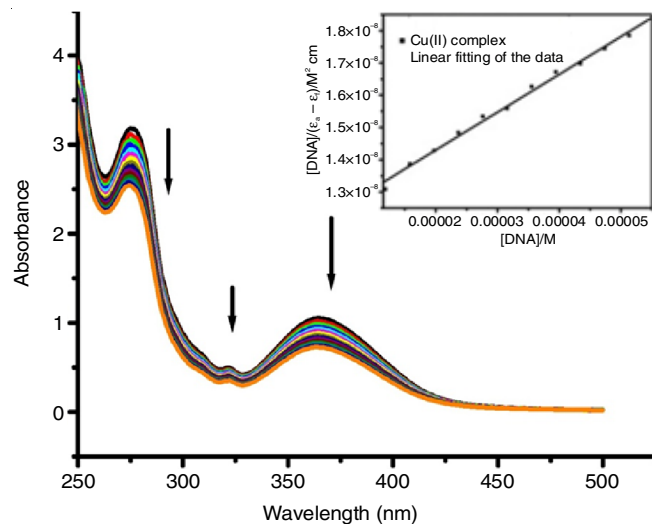

Fig. 8.   Absorption spectra of complex (**1**) (1.07×10^{-4} M) in Tris-buffer (pH =7.2) with CT-DNA (0–5.92×10^{-5} M). The arrow displays the absorbance changes with increase in DNA concentration and inset: sketch of $[DNA]/(\varepsilon_a - \varepsilon_f)$ *vs.* [DNA] for complex (**1**)
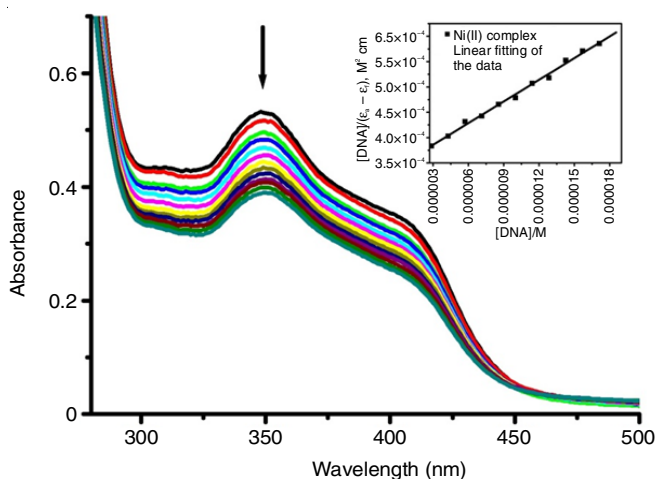
Fig. 9. Absorption spectra of complex (**2**) (4.83×10^{-5} M) in Tris-buffer (pH = 7.2) with CT-DNA ($0–1.71 \times 10^{-5}$ M). The arrow displays the absorbance changes with increase in DNA concentration and inset: sketch of [DNA]/($\varepsilon_a - \varepsilon_f$) *vs.* [DNA] for complex (**2**)
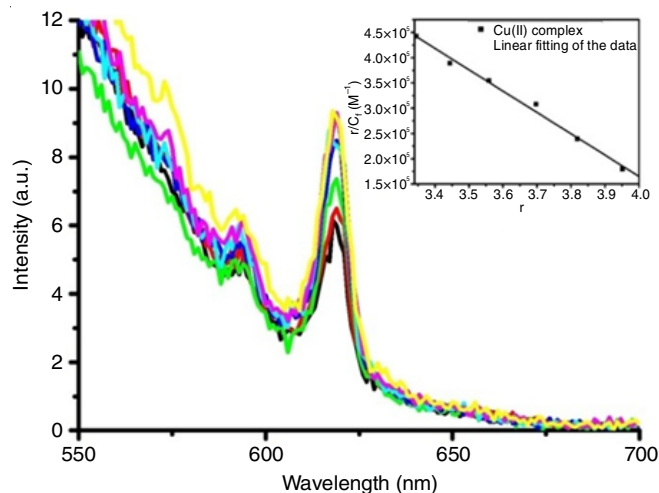

Fig. 10. Represents enhancement emission spectra of complex **1** (1.07×10^{-4} M) with CT-DNA (3.94×10^{-6} M $- 4.73 \times 10^{-5}$ M). Inset: Scatchard plot of complex **1**. Black one represents in absence and others in the participation of CT-DNA in buffer at pH = 7.2

Luminescence measurements

Emission titration: The emission spectral study was performed by titration at a fixed concentration of complex **1** (1.07×10^{-4} M) with increasing concentration of CT-DNA (3.94×10^{-6} M $- 4.737 \times 10^{-5}$ M) at room temperature in a buffer. Experimental data are analyzed by plotting r/C_f *versus* r using the Scatchard eqns 2 and 3 [49]. Here, r stands for the ratio of concentration of the bound compound, C_b to total available binding sites of CT-DNA, [DNA]$_t$ over the course of titration and C_b is evaluated using eqn 2:

$$C_b = C_t \times \left\{ \frac{(F - F^o)}{(F^{max} - F^o)} \right\} \qquad (2)$$

$$\frac{r}{C_f} = n.K_b - r.K_b \qquad (3)$$

where C_t, F, F^o, F^{max}, C_f, n and K_b represent total compound concentration, observed fluorescence emission intensity at specified DNA concentration, intensity in the failing of DNA, fluorescence of the totally bound compound, free compound concentration, binding site number, and binding constant in M^{-1} acquired as a negative slope, respectively. It was found to be 4.21×10^{-5} M $^{-1}$ and the spectrum is presented in Fig. 10.

Complex **1** shows an emission in DMSO at a maximum wavelength of about 617 nm ($\lambda_{ex} = 275$ nm) and enhancement in emission spectra was make out. The result could be set down to changing in the environment from polar to non-polar inside the DNA helix and amount to penetrate in this hydrophobic medium by the complex. In such medium, restricts the mobility of complex, leading to a dwindle of vibrational modes of relaxation and keep away from the lessen effects by solvent molecules [50].

Ethidium bromide (EB) competition study: Ethidium bromide displacement experiment was performed to an EB-DNA adduct by appending an increasing amount of the complexes and a classical Stern-Volmer equation [51] has been applied to calculate the K_{sv}, Stern-Volmer constant used as a binding quantifier of CT-DNA-complex obtained when plotting I_o/I against r.

$$\frac{I_o}{I} = 1 + K_{sv}.r \qquad (4)$$

where, I_o and I denote fluorescence intensities in the non-involvement and involvement of the complexes, respectively and r, the ratio of complex concentration to DNA concentration. EB itself has an emission at 616 nm in the buffer. An enhancement in emission intensity has observed when it is intercalated with the adjacent base pairs of DNAs. In most, an introduction of a second molecule to the EB-DNA adduct, a quenching phenomenon was observed which could be related in consequence of either replacing the bound EB from by decreasing the binding sites number of and/or by gaining the excited state electron of the EB *via* a photoelectron transfer mechanism [52]. The same phenomenon was observed in the complex **2** but an opposite trend in the complex **1**. In complex **1**, there is an increase in emission intensity in the presence of EB-DNA. Hence, a classical Stern-Volmer equation applied only in the complex **2** to assess the quenching effect. Fig. 11 represents the fluorescence emission spectra of EB bound to DNA both in the non-company and company of the complexes in different concentrations. The value of Stern-Volmer constant, K_{sv} for complex **2** is 4.26.

Cyclic voltammetry analysis: In a single compartmental cell containing a three-electrode system which composed of a glassy carbon working electrode, Pt-wire auxiliary electrode and an Ag/AgNO$_3$ as reference electrode, the electrochemical evaluations were achieved within +0.6 V to -1.4 V at a 0.01 V/s scan rate in *tris*-buffer (pH = 7.2) at room temperature. A supporting electrolyte, TBAB (0.1M) in double-distilled water was employed. The change in the electrochemical response of the complexes, at fixed concentrations, has checked in absence as well as the presence of varying CT-DNA concentration. Cyclic voltammograms of the complexes (**1-2**) in the absence as well as the presence of CT-DNA are shown in Fig. 12. The complex **1** shows one cathodic ($E_{pc} = -0.738$ V) and one anodic peak ($E_{pa} = -0.371$ V) along with peak separation ($\Delta E_p = 0.367$ V) and peak current ratio ($I_{pa}/I_{pc} = 0.472$). These value implies an
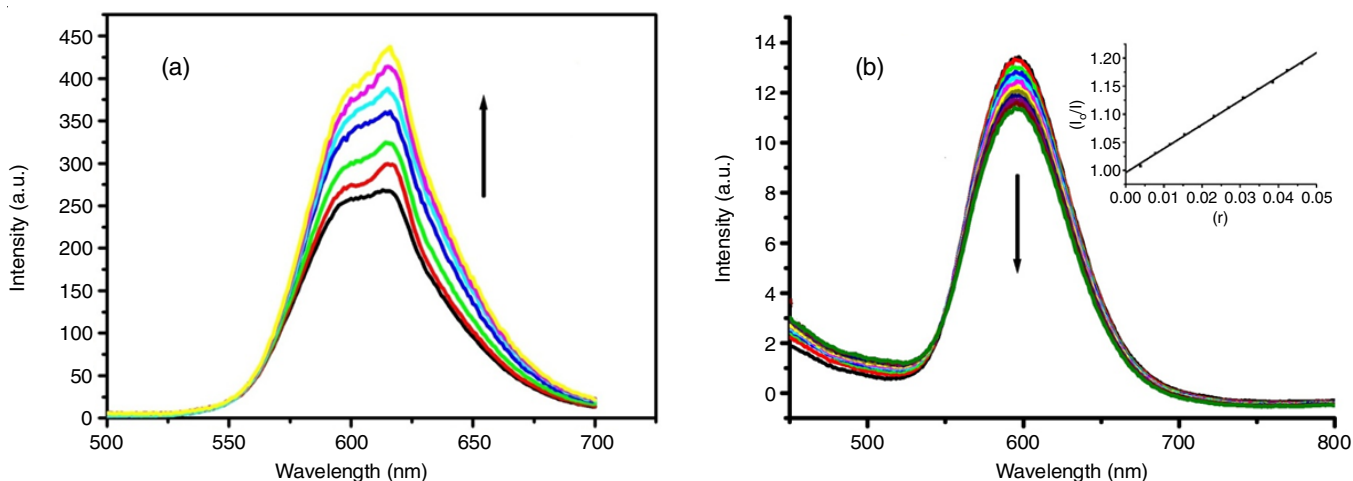
Fig. 11. (a) Emission spectra of CT-DNA-EB adduct (1.33×10^{-6} M: 1.33×10^{-6} M) in attending the complex (**1**) ($1.71 \times 10^{-6} - 2.4 \times 10^{-5}$ M) and (b) emission spectra of CT-DNA-EB adduct (6.5×10^{-6} M: 6.5×10^{-6} M) in the company of complex (**2**) ($0.025 \times 10^{-6} - 0.275 \times 10^{-6}$ M) along with Stern-Volmer plot. Variation in the emission intensity when raised in complex concentration has indicated *via* the arrows
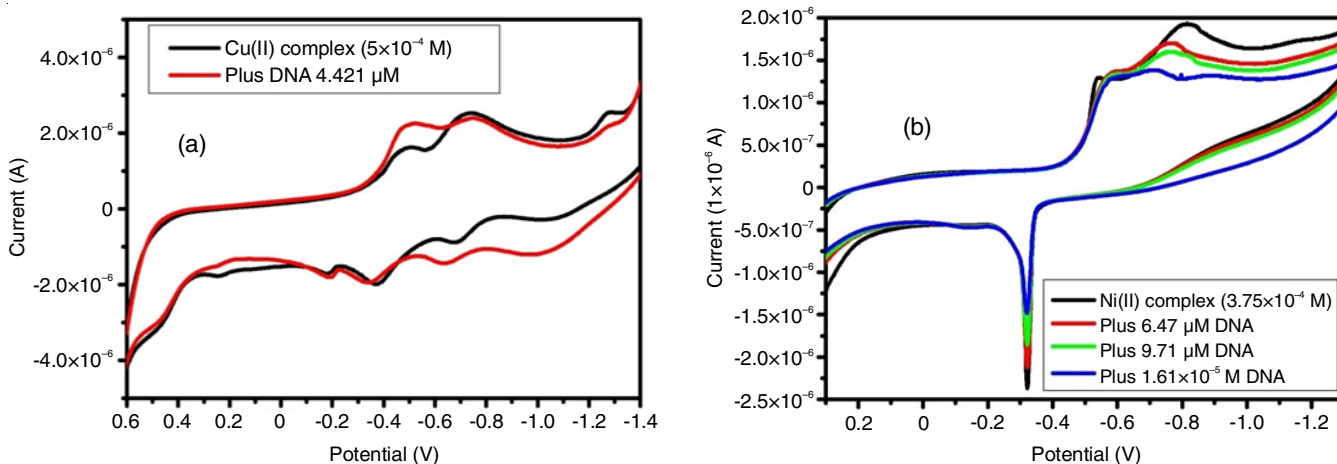

Fig. 12. Cyclic voltammogram of complexes (**1**) and (**2**) in Tris-buffer (pH = 7.2) in the absence and presence of CT-DNA

TABLE-3
ELECTROCHEMICAL RESULTS OF THE COMPLEXES IN THE ABSENCE AS WELL AS PRESENCE OF CT-DNA

Complex	Redox couple	E_{pc} (V)		E_{pa} (V)		ΔE_p (V)		$E_{1/2}$ (V)	
		Free	Bound	Free	Bound	Free	Bound	Free	Bound
1	Cu(II)/Cu(I)	-0.738	-0.755	-0.371	-0.340	0.367	0.415	-0.554	-0.547
2	Ni(II)/Ni(I)	-0.816	-0.765	-0.322	-0.322	0.494	0.443	-0.569	-0.543

$E_{1/2} = \frac{1}{2}(E_{pc} + E_{pa})$, $\Delta E_p = E_{pa} - E_{pc}$.

irreversible redox couple Cu(II)/Cu(I) since $\Delta E_p > 59$ mV for one electron diffusion and $I_{pa}/I_{pc} < 1$. The cathodic peak shifts to a more negative value ($E_{pc} = -0.755$ V), whereas an anodic peak to a more positive value ($E_{pa} = -0.340$ V) in presence of CT-DNA.

For complex **2**, the cathodic peak ($E_{pc} = -0.816$ V) shifts to a more positive value ($E_{pc} = -0.765$ V), while anodic peak ($E_{pa} = -0.322$ V) appeared at the same value in presence of CT-DNA. Experimental values are presented in Table-3. A positive shift in formal potential E° (or voltammetric $E_{1/2}$) and a decrease in current intensity in both complexes in presence of CT-DNA have confirmed the complexes that interact with CT-DNA and binds in an intercalative mode [53].

Viscosity measurements: Viscosity measurements of the complexes were carried out on an Oswald viscometer keeping in a thermostat water-bath at 25 ºC by adding an increasing amount of the complexes to a fixed concentration of DNA. Experimental data are presented by plotting $(\eta/\eta_o)^{1/3}$ *versus* [Q]/[DNA] = R, where η, η_o and [Q] represents viscosities of the DNA in the available, non-available of complexes, and complex concentration, respectively. The values of η and η_o were obtained using the following equation:

$$\eta = \frac{(t - t_o)}{t_o} \qquad (5)$$

where t_o and t are flow times of buffer alone and DNA containing complexes respectively. Also, the ratio of η and η_o gives

the relative viscosities of DNA [54]. It is known that when a complex interacts with DNA in intercalating mode causes an increase in viscosity, an electrostatic binding mode results in a decrease and a groove binding results a little or no effect on DNA viscosity [55]. A graph of relative viscosity $(\eta/\eta_o)^{1/3}$ *versus* [compound]/[DNA] is shown in Fig. 13. The effects on the relative viscosity of CT-DNA could be observed from this graph when the concentration of the complexes has increased. Thus, both the compounds bind to CT-DNA in an intercalative mode.
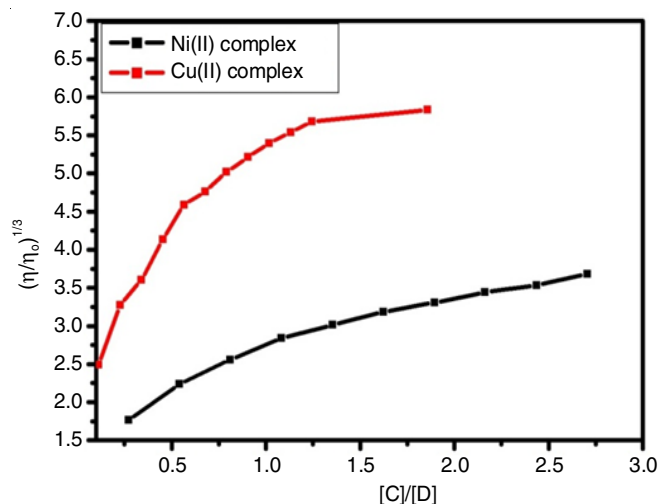

Fig. 13. Change in relative specific viscosity of CT-DNA (0.80×10^{-4} M for **1**; 3.08×10^{-5} M for **2**) in presence of the complexes **1** (9.09×10^{-6} – 1.49×10^{-4} M) and **2** (8.33×10^{-6} – 8.33×10^{-5} M) in Tris-buffer (pH = 7.2) at 25 °C

Conclusion

Complexes **1** and **2** crystallize at monoclinic and triclinic unit cells, respectively. Schiff base ligand participates in the formation distorted square planar complexes by contributing ONNO donor atoms. Magnetic, electronic and conductance values were in good agreement with the proposed structures. From the thermal analysis, it has inferenced about the lacking of lattice as well as coordinated water molecules in complexes **1** and **2**. Complex **1** is photo-active while complex **2** inactive. Both complexes bind to CT-DNA primarily by an intercalative binding mode. Complex **2** has a more pronounced effect in binding than complex **1**.

Supplementary materials

CCDC 1821322 available the accessory crystallographic data information of complex (**1**). These data can be viewed and downloaded in free of cost at www.ccdc.cam.ac.uk/ data_request/cif

CONFLICT OF INTEREST

The authors declare that there is no conflict of interests regarding the publication of this article.

REFERENCES

1. Q.L. Zhang, B.X. Zhu, L.F. Lindoy and G. Wei, *Inorg. Chem. Commun.*, **11**, 678 (2008);
https://doi.org/10.1016/j.inoche.2008.03.006
2. B. Miroslaw, B. Cristóvão and Z. Hnatejko, *Molecules*, **23**, 1761 (2018);
https://doi.org/10.3390/molecules23071761
3. A. Datta, K. Das, C. Massera, J.K. Clegg, C. Sinha, J.H. Huang and E. Garribba, *Dalton Trans.*, **43**, 5558 (2014);
https://doi.org/10.1039/c4dt00189c
4. M.L. Sundararajan, T. Jeyakumar, J. Anandakumaran and B.K. Selvan, *Spectrochim. Acta A Mol. Biomol. Spectrosc.*, **131**, 82 (2014);
https://doi.org/10.1016/j.saa.2014.04.055
5. S.K. Tadavi, A.A. Yadav and R.S. Bendre, *J. Mol. Struct.*, **1152**, 223 (2018);
https://doi.org/10.1016/j.molstruc.2017.09.112
6. V.M.R. Garia, P.E. Martinez, N.P. Rodriguez and B.N. Martinez, *Quim. Hoy Chem. Sci.*, **4**, 30 (2012).
7. E.K. Baran and S.B. Yasar, *J. Anal. Chem.*, **68**, 788 (2013);
https://doi.org/10.1134/S1061934813090074
8. P.K. Bhattacharya, *Proc. Indian Acad. Sci.*, **102**, 247 (1990).
9. P. Gawryszewska and Lisowski, *J. Inorg. Chim. Acta.*, **383**, 220 (2012);
https://doi.org/10.1016/j.ica.2011.11.012
10. D.M. Boghaei, M. Behzad and A. Bezaatpour, *J. Mol. Catal. A Chem.*, **241**, 1 (2005);
https://doi.org/10.1016/j.molcata.2005.06.064
11. P.A. Vigato and S. Tamburini, *Coord. Chem. Rev.*, **248**, 1717 (2004);
https://doi.org/10.1016/j.cct.2003.09.003
12. P.A. Vigato, S. Tamburini and L. Bertolo, *Coord. Chem. Rev.*, **251**, 1311 (2007);
https://doi.org/10.1016/j.ccr.2006.11.016
13. W. Radecka-Paryzek, V. Patroniak and J. Lisowski, *Coord. Chem. Rev.*, **249**, 2156 (2005);
https://doi.org/10.1016/j.ccr.2005.02.021
14. M.R. Maurya, S. Dhaka and F. Avecilla, *Polyhedron*, **67**, 145 (2014);
https://doi.org/10.1016/j.poly.2013.08.050
15. K.I. Smith, L.L. Borer and M.M. Olmstead, *Inorg. Chem.*, **42**, 7410 (2003);
https://doi.org/10.1021/ic034640p
16. A. Yardan, Y. Yahsi, H. Kara, A. Karahan, S. Durmus and R. Kurtaran, *Inorg. Chim. Acta.*, **413**, 55 (2014);
https://doi.org/10.1016/j.ica.2014.01.006
17. M.R. Maurya, N. Chaudhary, F. Avecilla and I. Correia, *J. Inorg. Biochem.*, **147**, 181 (2015);
https://doi.org/10.1016/j.jinorgbio.2015.01.012
18. M.R. Maurya, M. Bisht, N. Chaudhary, F. Avecilla, U. Kumar and H.F. Hsu, *Polyhedron*, **54**, 180 (2013);
https://doi.org/10.1016/j.poly.2013.02.036
19. N. Gao, H. Li, Q. Li, J. Liu and G. Luo, *J. Inorg. Biochem.*, **105**, 283 (2011);
https://doi.org/10.1016/j.jinorgbio.2010.09.014
20. M. Mitra, A.K. Maji, B.K. Ghosh, P. Raghavaiah, J. Ribas and R. Ghosh, *Polyhedron*, **67**, 19 (2014);
https://doi.org/10.1016/j.poly.2013.08.064
21. N.S. Devi, L.J. Singh, S.P. Devi, R.K.B. Singh, R.K.H. Singh, B. Rajeswari and R.M. Kadam, *J. Mol. Struct.*, **1076**, 411 (2014);
https://doi.org/10.1016/j.molstruc.2014.08.005
22. R.K.B. Devi, S.P. Devi, R.K.B. Singh, R.K.H. Singh, T. Swu, W.R. Devi and C.B. Singh, *J. Coord. Chem.*, **67**, 891 (2014);
https://doi.org/10.1080/00958972.2014.902449
23. W.B. Devi, R.K.B. Singh, J.P. Jasinski and J.A. Golen, *Inorg. Chem. Commun.*, **21**, 163 (2012);
https://doi.org/10.1016/j.inoche.2012.05.006
24. W.B. Devi and R.K.B. Singh, *Int. J. Scient. Res.*, **2**, 312 (2013).

25. O. U-wang, R.K.B. Singh, W.B. Devi, U.I. Singh, R.K.B. Devi, O.B. Devi, Ramina, Th. Surchandra Singh and T. Swu, *Chem. Sci. Int. J.*, **26**, 1 (2019);
https://doi.org/10.9734/CSJI/2019/v26i230091

26. G.M. Sheldrick, *Acta Cryst. C*, **71**, 3 (2015);
https://doi.org/10.1107/S2053229614024218

27. O.V. Dolomanov, L.J. Bourhis, R.J. Gildea, J.A.K. Howard and H. Puschmann, *J. Appl. Cryst.*, **42**, 339 (2009);
https://doi.org/10.1107/S0021889808042726

28. W.J. Geary, *Coord. Chem. Rev*., **7**, 81 (1971);
https://doi.org/10.1016/S0010-8545(00)80009-0

29. M.R. Malachowski, J. Carden, M.G. Davidson, W.L. Driessen and J. Reedijk, *Inorg. Chim. Acta*, **257**, 59 (1997);
https://doi.org/10.1016/S0020-1693(96)05448-5

30. E.B. Seena, N. Mathew, M. Kuria-Kose and M.R.P. Kurup, *Polyhedron*, **27**, 1455 (2008);
https://doi.org/10.1016/j.poly.2008.01.020

31. D.M. Boghaei and M. Gharagozlou, *Spectrochim. Acta A Mol. Biomol. Spectrosc.*, **67**, 944 (2007);
https://doi.org/10.1016/j.saa.2006.09.012

32. M.R. Maurya, S. Dhaka and F. Avecilla, *Polyhedron*, **67**, 145 (2014);
https://doi.org/10.1016/j.poly.2013.08.050

33. K. Mohammadi, M. Niad and A. Irandoost, *Spectrochim. Acta A Mol. Biomol. Spectrosc.*, **107**, 145 (2013);
https://doi.org/10.1016/j.saa.2013.01.035

34. M.B. Halli and V.B. Patil, *J. Coord. Chem.*, **64**, 3740 (2011);
https://doi.org/10.1080/00958972.2011.630730

35. R.N. Patel, K.K. Shukla, A. Singh, M. Choudhary, D.K Patel, J. Niclos-Gutierrez and D. Choquesillo-Lazarte, *J. Coord. Chem.*, **63**, 3648 (2010);
https://doi.org/10.1080/00958972.2010.515985

36. S. Biswas and A. Ghosh, *Indian J. Chem.*, **50A**, 1356 (2011).

37. D.N. Sathyanarayana, Electronic Absorption Spectroscopy and Related Technique, Universities Press India Limited, edn 1, p. 244 (2001);

38. A.A. Kitos, D.P. Giannopoulos, C. Papatriantafyllopoulou, L. Cunha-Silva and S.P. Perlepes, *Inorg. Chem. Commun.*, **64**, 53 (2016);
https://doi.org/10.1016/j.inoche.2015.12.015

39. L. Yang, D.R. Powell and R.P. Houser, *Dalton Trans*., 955 (2007);
https://doi.org/10.1039/b617136b

40. A. Okuniewski, D. Rosiak, J. Chojnacki and B. Becker, *Polyhedron*, **90**, 47 (2015);
https://doi.org/10.1016/j.poly.2015.01.035

41. D. Rosiak, A. Okuniewski and J. Chojnacki, *Polyhedron*, **146**, 35 (2018);
https://doi.org/10.1016/j.poly.2018.02.016

42. P. Kavitha, M. Saritha and K.L. Reddy, *Spectrochim. Acta A Mol. Biomol. Spectrosc*., **102**, 159 (2013);
https://doi.org/10.1016/j.saa.2012.10.037

43. B.J.M.L. Ferreira, P. Brandão, M. Meireles, F. Martel, A. Correia-Branco, D.M. Fernandes, T.M. Santos and V. Félix, *J. Inorg. Biochem.*, **161**, 9 (2016);
https://doi.org/10.1016/j.jinorgbio.2016.04.026

44. N. Raman, K. Pothiraj and T.H. Baskaran, *J. Mol. Struct*., **1000**, 135 (2011);
https://doi.org/10.1016/j.molstruc.2011.06.006

45. R.K. Gupta, G. Sharma, R. Pandey, A. Kumar, B. Koch, P-Z. Li, Q. Xu and D.S. Pandey, *Inorg. Chem.*, **52**, 13984 (2013);
https://doi.org/10.1021/ic401662d

46. T. Kiran, V.G. Prasanth, M.M. Balamurali, C.S. Vasavi, P. Munusami, K.I. Sathiyanarayanan and M. Pathak, *Inorg. Chim. Acta*, **433**, 26 (2015);
https://doi.org/10.1016/j.ica.2015.04.033

47. P. Kalaivani, C. Umadevi, R. Prabhakaran, F. Dallemer, P.S. Mohan and K. Natarajan, *Polyhedron*, **80**, 97 (2014);
https://doi.org/10.1016/j.poly.2014.02.011

48. O. U-Wang, R.K.B. Singh, W.B. Devi, U.I. Singh, R.K.B. Devi, O.B. Devi, Ramina and Toka Swu, *Inorg Nano-Met Chem.*, **49**, 363 (2019);
https://doi.org/10.1080/24701556.2019.1661457

49. Y. Li, Y. Zheng-Yin and W. Ming-Fang, *J. Fluoresc.*, **20**, 891 (2010);
https://doi.org/10.1007/s10895-010-0635-z

50. M.R. Shorkaei, Z. Asadi and M. Asadi, *J. Mol. Struct*., **1109**, 22 (2016);
https://doi.org/10.1016/j.molstruc.2015.12.070

51. F. Arjmand, I. Yousuf, T.B. Hadda and L. Toupet, *Eur. J. Med. Chem.*, **81**, 76 (2014);
https://doi.org/10.1016/j.ejmech.2014.04.080

52. S.P. Devi, R.K.B. Devi, N.S. Devi, L.J. Singh and R.K.H. Singh, *Polyhedron*, **47**, 1 (2012);
https://doi.org/10.1016/j.poly.2012.08.033

53. A. Gubendran, M.P. Kesavan, S. Ayyanaar, L. Mitu, P. Athappan and J. Rajesh, *Spectrochim. Acta A Mol. Biomol. Spectrosc.*, **181**, 39 (2017);
https://doi.org/10.1016/j.saa.2017.03.031

54. T.H. Chandrasekar and N. Raman, *J. Mol. Struct*., **1116**, 146 (2016);
https://doi.org/10.1016/j.molstruc.2016.02.102

55. I. Yousuf and F. Arjmand, *J. Photochem. Photobiol. B*, **164**, 83 (2016);
https://doi.org/10.1016/j.jphotobiol.2016.09.016